CHEMISTRY
A EUROPEAN JOURNAL

DOI: 10.1002/chem.201001358

Mechanistic Investigation of Organolanthanide-Mediated Hydroamination of Conjugated Aminodienes: A Comprehensive Computational Assessment of Various Routes for Diene Activation

Sven Tobisch*[a]

Abstract: The present computational mechanistic study comprehensively explores alternative scenarios for activation of the amine-linked diene C=C linkage toward C–N ring closure in intramolecular hydroamination of a prototypical aminodiene by a well-characterised lanthanocene–amido catalyst. Firstly, the non-insertive mechanism by Scott featuring ring closure with concomitant amino proton delivery onto the diene unit has been explored and key features have been defined. This scenario has been compared with the classical stepwise insertion mechanism that involves rapid substrate association/dissociation equilibria for the **3t**-S1 resting state and also for azacycle intermediates **4s**, **4a**, facile and reversible exocyclic migratory diene insertion into the La–N(amido) σ-bond, linked to turnover-limiting La–C azacycle aminolysis. The Ln–N σ-bond insertive mechanism prevails for the examined intramolecular hydroamination of (4*E*,6)-heptadienylamine **1t** by $[Cp^*_2La–CH(TMS)_2]$ starting material **2**.The following aspects are in support of this mechanism: 1) the derived rate law is consistent with the observed empirical rate law; 2) the assessed effective barrier for turnover-limiting aminolysis does agree remarkably well with empirically determined Eyring parameters; 3) the ring-ether double-bond selectivity is consistently elucidated. This study reveals that the non-insertive mechanism is not achievable for the particular lanthanocene–amido catalyst and furthermore cannot account for the observed product spectrum. Notwithstanding of these findings, the non-insertive mechanism cannot be discarded a priori for intramolecular aminodiene hydroamination. Spatial demands around the lanthanide centre influence the two mechanisms differently. The Ln–N σ-bond insertive mechanism critically relies on a sufficiently accessible lanthanide and enhanced encumbrance renders cyclisation and aminolysis steps less accessible kinetically. It contrasts with the non-insertive mechanism, where greater lanthanide protection has a rather modest influence. The present study indicates that the non-insertive mechanism would prevail if the lanthanide centre were to be protected effectively against C=C bond approach. Notably, a different product spectrum would be expected for aminodiene hydroamination following the insertive or non-insertive route.

Keywords: density functional calculations · dienes · hydroamination · lanthanides · reaction mechanisms

Introduction

Catalytic hydroamination (HA), that is, the direct addition of N–H bonds across multiple carbon–carbon linkages is a valuable synthetic methodology for regiospecific C–N bond formation and is attracting as such considerable interest in both academia and industry.[1] Intramolecular HA represents an efficient, concise and fully atom-economical route to functionalised nitrogen hetereocycles. Organolanthanide complexes are known to be highly active catalysts for this process, their versatility has been broadly demonstrated.[1k,2]

The rational design of improved catalysts relies on the precise understanding of the underlying mechanism. Unlike the cyclohydroamination mediated by late transition-metal complexes, where a multitude of ways to activate the substrate have reported over the years,[3] for organolanthanides it is commonly believed and substantiated by both experimental[1k] and computational evidence[4] that interaction with the electropositive lanthanide centre activates an unsaturated C–C unit towards nucleophilic amido attack. This classical insertive mechanism[2a,b] comprises of C–N bond formation through 1,2-insertion of a C=C linkage into the

[a] Dr. S. Tobisch
University of St Andrews, School of Chemistry
Purdie Building, North Haugh, St Andrews
Fife KY16 9ST (UK)
Fax: (+44) 1797-383-652
E-mail: st40@st-andrews.ac.uk

Supporting information for this article is available on the WWW under http://dx.doi.org/10.1002/chem.201001358.

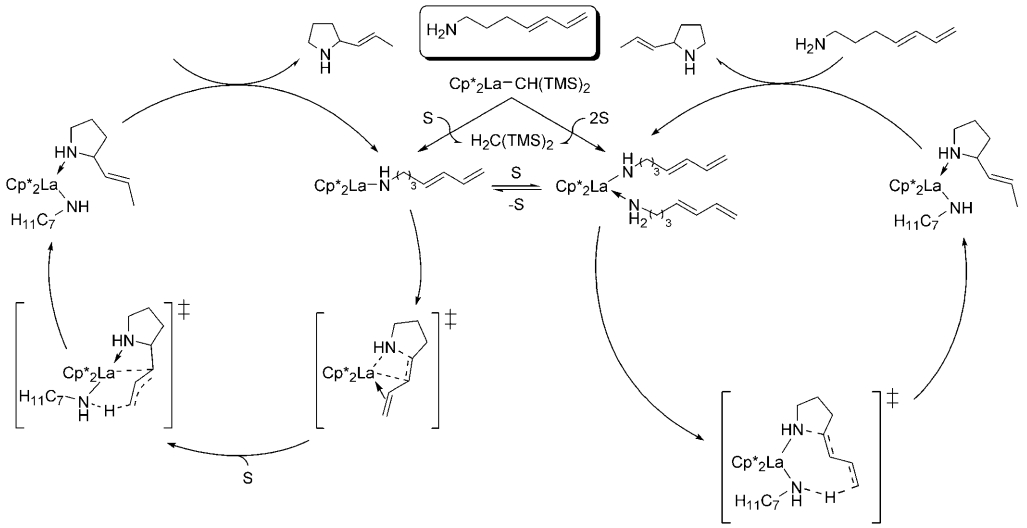

Scheme 1. Plausible mechanistic scenarios for organolanthanide-assisted intramolecular hydroamination of aminodienes. Activation of the diene unit towards nucleophilic amido attack does proceed either by interaction with the electropositive Ln centre (insertive mechanism, left) or by amino proton delivery (non-insertive mechanism, right).

Ln–N amido σ-bond to be followed by Ln–C azacycle protonolysis. Recently, Scott[5] has suggested another plausible scenario, featuring amino proton delivery to activate an unsaturated C–C unit and concurrent ring closure proceeding outside of the immediate proximity of the Ln centre. Thus, according to this non-insertive mechanism (Scheme 1, right), cycloamines are generated in a concerted fashion commencing from the Ln–amido catalyst species. However, this proposal has not been substantiated thus far for any substrate class by either experimental or computational mechanistic studies. Whilst observed reactivity/selectivity patterns[1k] and computational examination,[4] provided firm evidence in support of an operating insertive mechanism for the various substrate classes (Scheme 1, right), the primary KIE observed in aminoalkene HA[2b] cannot be easily rationalised in the context of this mechanism.[6] Which of the alternative mechanisms dominates may depend on factors including the accessibility of the Ln centre and the identity of the C–C unsaturation.

Herein is reported a comprehensive computational assessment of alternative mechanisms for aminodiene cyclohydroamination mediated by a well-characterised lanthanocene–amido catalyst[7] as a prototypical organolanthanide system with a noticeable steric encumbrance around the Ln centre. The $[(\eta^5\text{-Cp}^*)_2\text{La–CH(TMS)}_2]$ starting material **2**, which is readily transformed by substrate aminolysis into the Cp^*_2La–amido catalyst species, transforms (4*E*,6)-heptadienylamine substrate **1t** with complete regioselectivity to pyrrolidines **P6**, whilst piperidine **P7** is not among the products (Scheme 2).[7]

The thermodynamically favoured pyrrolidines **P6a/b** bearing an internal (*E*/*Z*) double bond are almost exclusively formed with good *E* double bond selectivity. The DFT method has been employed as an established and predictive means to aid mechanistic understanding; the particular value of such methods for unravelling intricacies in hydroamination catalysis has been demonstrated previously by several groups.[4,8–12] Plausible mechanistic scenarios employing $[Cp^*_2La\text{–amido–(substrate)}_n]$ as the active catalyst species involving activation of the unsaturated diene unit towards nucleophilic amido attack by either the electropositive Ln centre (insertive mechanism, Scheme 1, left) or by amino proton delivery (non-insertive mechanism, Scheme 1, right) have been examined. No structural simplification of any of the key species has been imposed. The employed reliable DFT methodology has simulated the authentic reaction conditions adequately. Whilst the discussion herein is focused exclusively on the most accessible pathways, a complete account of all the scrutinised species is given in the Supporting Information.

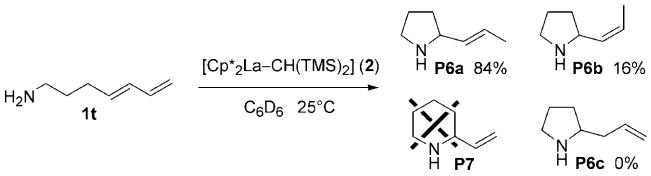

Scheme 2. Intramolecular HA of aminodiene **1t** mediated by $[Cp^*_2La\text{–CH(TMS)}_2]$.

Herein is presented sound evidence that migratory diene insertion into the La–N amido σ-bond in the substrate-free La–amido catalyst species, followed by turnover-limiting aminolysis of the azacycle's allylic tether is the most accessible route for the particular lanthanocene catalyst. The mechanistic path for cycloamine formation in a single step via non-insertive cyclisation with concurrent amino proton delivery onto the diene unit is found to be not accomplishable. Firstly, a TS structure for the direct generation of the major pyrrolidines **P6a/P6b** could not be located because protonation at the remote diene–C^8 appears not to activate the diene–C^5 efficiently toward nucleophilic amido attack.

Secondly, an alternative pathway that starts with formation of **P6c** and its complete transformation into **P6a**/**P6b** thereafter through product reinsertion and concomitant allyl isomerisation proved to be inaccessible. The assessed smooth energy profile for the insertive mechanism is consonant with the observed kinetic data and the empirical rate law. Although not traversable for the particular lanthanocene–amido catalyst, the non-insertive mechanism cannot be discarded a priori in organolanthanide-mediated intramolecular HA of aminodienes and may perhaps be operational for particularly designed ligand architectures featuring a less accessible lanthanide centre. The detailed insights into the structure–reactivity relationships of the various mechanistic scenarios provided in this study will undoubtedly broaden our understanding of hydroamination catalysis.

Results and Discussion

The examination of alternative mechanistic scenarios will focus exclusively on pathways that lead to pyrrolidines **P6**. The observed complete regioselectivity of ring closure has already been consistently elucidated in a previous computational study.[4d] We start with an assessment of the various forms of the Cp^*_2La–amidodiene catalyst species[13] and examine which of them does participate in the non-insertive mechanism (Scheme 3). Major mechanistic features of the Ln–N σ-bond insertive mechanism (Scheme 5), which have been unveiled in a previous computational study[4d,13] but extended by the present study, are summarised next. A critical comparison of the mechanistic scenarios follows thereafter. The aptitude of the active catalyst species to bind substrate molecules, thereby perhaps limiting the accessibility of the Ln centre for the diene unit may profoundly influence which of the mechanisms will dominate. To this end, the present study devotes particular attention to what role substrate molecules play in the various steps.

The non-insertive mechanism: Scheme 3 shows a plausible catalytic cycle for the generation of pyrrolidines **P6** from (4*E*,6)-heptadienylamine (**1t**) with $[Cp^*_2La{-}H(TMS)_2]$ (**2**) proceeding via the non-insertive mechanism. Starting material **2** becomes smoothly transformed into the Cp^*_2La–amidodiene compound,[4d] as *trans* (**t**) and *cis* (**c**) isomers of the diene fragment, through aminolysis at the La–$CH(TMS)_2$ bond by **1t**. The Cp^*_2La–amidodiene catalyst complex can exist in substrate-free forms (**3t**, **3c**) and as substrate adducts (**3t**-Sn, **3c**-Sn). The latter represent precursors for non-insertive exocyclic ring closure with concurrent amino proton delivery onto the diene unit to afford Cp^*_2La–cycloamine compound **6** in a single step, from which pyrrolidines are readily liberated to regenerate the catalytically competent Cp^*_2La–amidodiene complex and complete the cycle. Intramolecular proton transfer onto the substituted diene–C^6 centre in **3t**-S1 and **3c**-S1 furnishes 2-(prop-2-enyl)pyrrolidine (**P6c**). On the other hand, protonation of the terminal diene–C^8 centre gives rise to *E* and *Z* isomers of 2(prop-1-enyl)pyrrolidine **P6a** and **P6b**, respectively, when starting from **3t**-S1 and **3c**-S1, respectively.

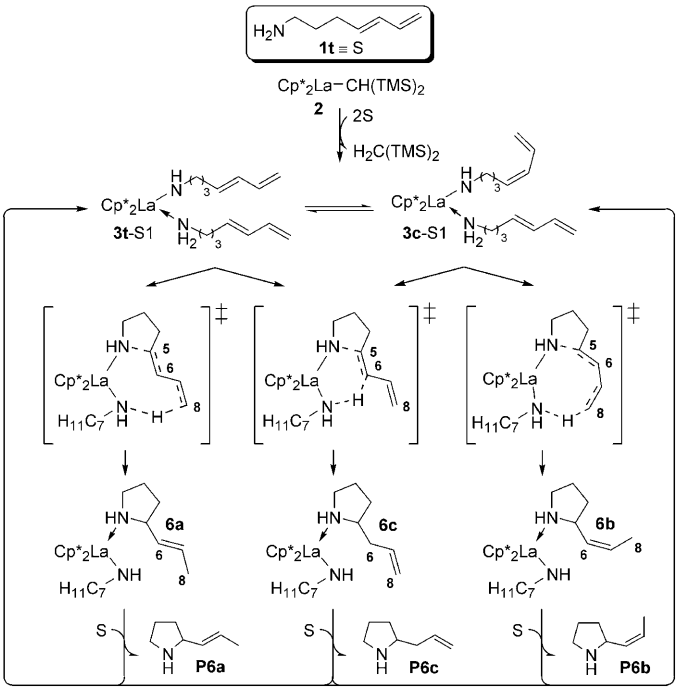

Scheme 3. General catalytic reaction course for organolanthanide-mediated intramolecular HA of aminodienes via the non-insertive mechanism to afford functionalised five-cycle amines, exemplified for **3**-S1 as the active catalyst species.[14]

We start with an examination of the various forms of the catalytically competent Cp^*_2La–amidodiene compound (Figures 1 and S1). The favourable substrate-free species is **3t**

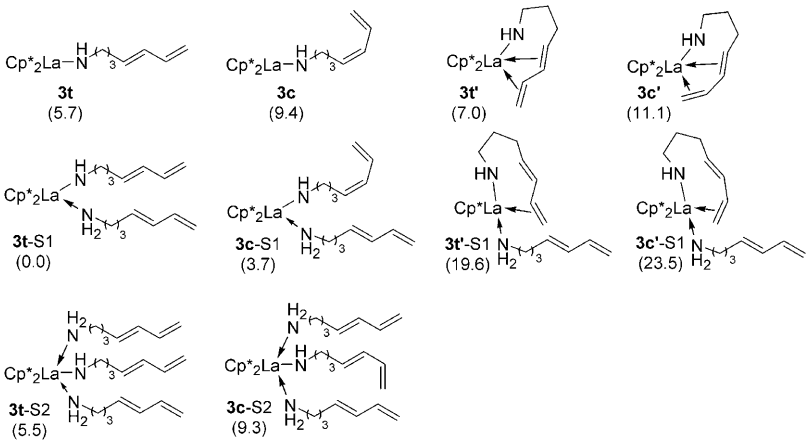

Figure 1. Various forms of the catalytically competent lanthanocene–amido compound.[15,17a]

with a mono-hapto amido-*trans*-diene group, whilst **3t′** in which the amidodiene unit forms a weak chelate by orienting the terminal diene double bond proximal to the La centre is only marginally less stable. A similar trend is observed for the corresponding, but thermodynamically disfavoured, *cis*-diene species **3c** and **3c′**. Conversion of the *trans*-diene unit into the *cis* isomer is kinetically easy ($\Delta G^{\neq} = 7.5$ kcal mol^{-1}). Up to two substrate molecules bind favourably on the catalyst complex, the stable adducts **3t**-S1 and **3t**-S2, the former of which is prevalent, feature a mono-hapto amidodiene unit (Figure 1). It comes as no surprise that for the sterically congested lanthanocene-amido complex an adduct **3t**-S3 with three associated substrate molecules could not be located. Moreover, the rather weak amidodiene chelate cannot compete for coordination to the La centre with the amine and therefore **3t′**-S1 is substantially above **3t**-S1, whilst a corresponding species **3t′**-S2 with two associated substrate molecules could not be located. The large energy gap ($\Delta G = 19.6$ kcal mol^{-1}) between **3t**-S1 and **3t′**-S1 clearly indicates a drastically reduced accessibility of the La centre for the diene unit in **3t**-S1 and even more so in **3t**-S2 when compared to the substrate-free species **3t**. Overall, the catalytically competent lanthanocene-amido compound is predominantly present as adduct **3t/c**-S1 (Figure 1) to enter the productive catalytic cycle.

Non-insertive ring closure with concurrent amino proton delivery: The most accessible pathways for the various branches shown in Scheme 3 are discussed in this section, whereas the full account of structural (see Figure S2, S3) and energy aspects (see Tables S1a, S1b)[16] of all the examined pathways can be found in the Supporting Information. The way the $C^5{=}C^6$ double bond is activated toward nucleophilic amido attack, thereby accomplishing C^5–N ring closure, distinguishes the branches; by proton delivery to either the adjacent diene–C^6 or the remote diene–C^8 centres. We start with an examination of the first case that leads to **6c** with **3t**-S1 or **3c**-S1 is the precursor. This process evolves through a TS structure that describes C^5–N bond formation with concurrent proton delivery from a La-coordinated, hence acidified, amine onto the adjacent diene–C^6 centre (Figure 2a). It features an almost accomplished ring closure, as seen by a rather short C^5–N distance of 1.72 Å, occurring outside of the immediate La proximity, together with vanishing N–H (1.24 Å) and emerging C–H (1.57 Å) bonds, which is indicative of an almost half-complete proton delivery. In stark contrast, a related TS structure for outer-sphere cyclisation with concurrent proton transfer onto the remote diene–C^8 centre could not be located. A closer look at the charge distribution depicted in Figure 3 provides a rationale. Protonation at the diene–C^6 polarises the adjacent C^5 centre favourably toward nucleophilic amido attack; whilst the accumulation of a positive partial charge at C^5 is less pronounced if the proton were delivered at the terminal diene–C^8. Thus, amino protonation at the remote C^8 centre is less effective to activate the diene unit for C–N bond formation,

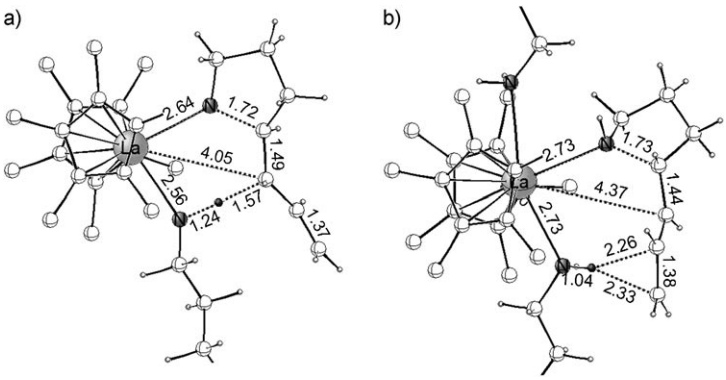

Figure 2. Located TS structure for concerted non-insertive cyclisation and amino proton delivery onto diene–C^6 in **3t**-S1 (a) and for outer-sphere cyclisation in **3t**-S2 (b), respectively.[18]

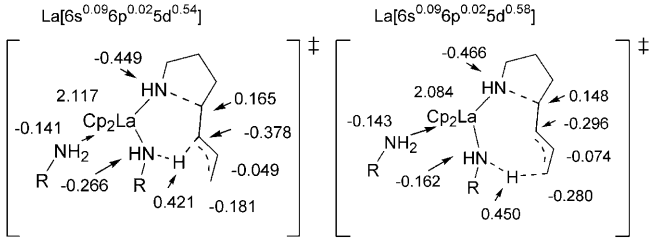

Figure 3. Charge distribution in the TS for non-insertive cyclisation with concurrent amino proton delivery onto diene–C^6 (left) and diene–C^8 (right) in **3t**-S2.[19] Brutto charges on individual atoms including bound hydrogens and orbital population for La, covering major contributions, are shown.

which may perhaps prevent the localisation of a concerted outer-sphere TS.

An additional associated substrate molecule, which could be either *trans* or *cis* disposed to the H-delivering amine (Scheme 4, the former of which is slightly favourable, see

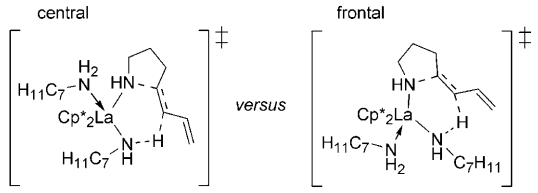

Scheme 4. Alternative trajectories for non-insertive C–N ring closure with concomitant amino proton delivery onto the diene unit (exemplified for diene C^6 centre) in **3t**-S2.

Table S1b)[16] does not affect principal characteristics of the process. Again, a TS structure for the conversion of **3**-S2 into **6c**-S1 in a single step does exist, whilst the TS for generation of **6a/c**-S1 via simultaneous outer-sphere cyclisation and diene–C^8 protonation in **3t/c**-S2 could not be located. Interestingly, for **3t/c**-S2, in which the two associated substrate molecules protect the La centre effectively against diene approach, an alternative TS structure has been found.

It describes an outer-sphere C–N ring closure without concomitant diene protonation, but having the emerging butenyl tether stabilised by close H contacts and the surrounding solvent, as represented by a polarisable continuum model (Figure 2b). It comes as no surprise that this trajectory has a substantial barrier as high as 37 kcal mol^{-1} (see Table S1b),[16] thus being not compatible with observed smooth catalysis, which is also higher than the barrier for **3t**-S2 → **6c**-S1 conversion (Figure 4).

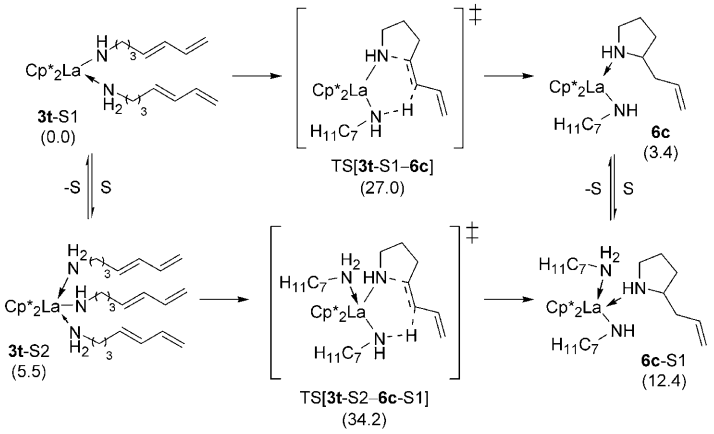

Figure 4. Most accessible pathways for non-insertive C–N ring closure with concurrent amino proton delivery onto the diene–C^6 centre in **3**-S1 and **3**-S2.[17]

The conversion of **3t**-S1 into **6c** has a barrier of 27.0 kcal mol^{-1} (Figure 4) when proceeding in a single step. Notably, an intrinsic barrier of similar magnitude ($\Delta G^{\neq} = 28.7$ kcal mol^{-1} relative to **3t**-S2)[16] has to overcome when commencing from **3t**-S2. It illustrates that a less accessible La centre, in contrast to insertive cyclisation (see below), is not a limiting factor here.

The insertive mechanism: The reaction cycle for intramolecular HA to proceed via the classical Ln–N σ-bond insertive mechanism is shown in Scheme 5. It comprises accessible pathways for all relevant steps that have been previously identified by computational examination.[4d] Migratory insertion of the C^5=C^6 diene double bond into the La–N amido σ-bond in the La–amido catalyst complex when proceeding through the exocyclic pathway gives rise to **4** bearing a 2-substituted five-membered azacycle tethered to an allylic functionality. Isomers **4s** and **4a** with a *syn*-η^3- and *anti*-η^3-butenyl–La functionality[20] are generated when commencing from **3t** (or **3t**-Sn) and **3c** (or **3c**-Sn), respectively, which are interconnected by allylic isomerisation. La–C bond aminolysis in **4** by **1t** affords first Cp*$_2$La–cycloamine compound **6**, from which the cycloamine is readily liberated to regenerate the catalytically competent La–amido complex and complete the cycle. Aminolysis at the La–C^8 bond affords **P6a**, **P6b**, when commencing from **4s** and **4a**, whilst intramolecular proton transfer onto the substituted C^6 centre in **4s** or **4a** gives rise to **P6c**.

The catalytically competent La–amido complex predominantly exists as adduct **3**-S1, but adduct **3**-S2 and the substrate-free species **3** are also present in rapid equilibria (Figure 1), whilst the encumbrance around the La centre makes the association of more than two substrate molecules rather unlikely (see above). Thus, exocyclic ring closure in **3**, **3**-S1, **3**-S2, (see Tables S2a–S2c)[16] subsequent intramolecu-

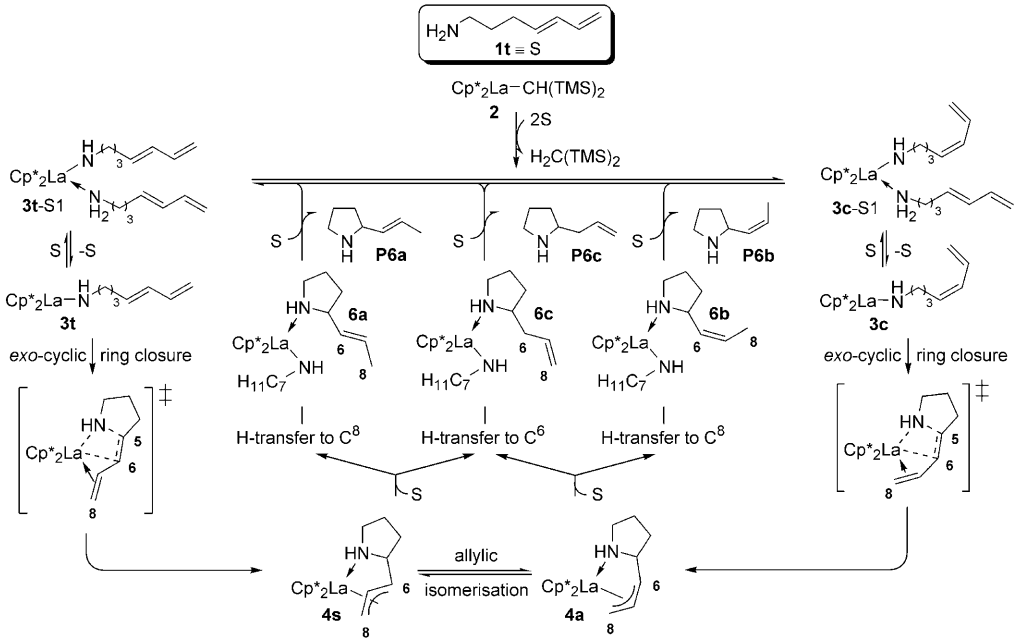

Scheme 5. Catalytic reaction course for organolanthanide-mediated intramolecular HA of aminodienes via the classical insertive mechanism to afford functionalised five-cycle amines, based on experimental[7] and computational[4d] mechanistic studies.[14]

lar proton transfer (see Tables S4a, S4b)[16] and isomerisation of the allylic tether in La-azacyle intermediate (see Tables S3a–S3c)[16] have been examined. A complete account of all studied pathways (see Figure S4–S8) can be found in the Supporting Information.

Migratory diene insertion into the La–N amido σ-bond: Considering the prevalent species **3**-S1, two trajectories are conceivable for insertive cyclisation (Scheme 6);[21] firstly, the frontal approach of the C=C linkage along the ring-centroid-La-ring-centroid bisector, and secondly, the lateral approach along the perpendicular to the ring-centroid-La-ring-centroid plane. The association of one substrate molecule disfavours close La–diene interactions as indicated by the substantial disparity in stability between **3t**-S1 and **3t′**-S1 species (Figure 1). The limited accessibility of the La centre due to one complexed amine molecule gives rise to a barrier of 21.2 kcal mol^{-1} for **3t**-S1 → **4s**-S1 insertive cyclisation (Figure 5) via the favourable frontal trajectory. An even larger barrier of 38.8 kcal mol^{-1} would have to be traversed for **3t**-S2 → **4s**-S2 ring closure via the central trajectory (Scheme 6), where two associated substrate molecules protect the La centre effectively from diene approach.

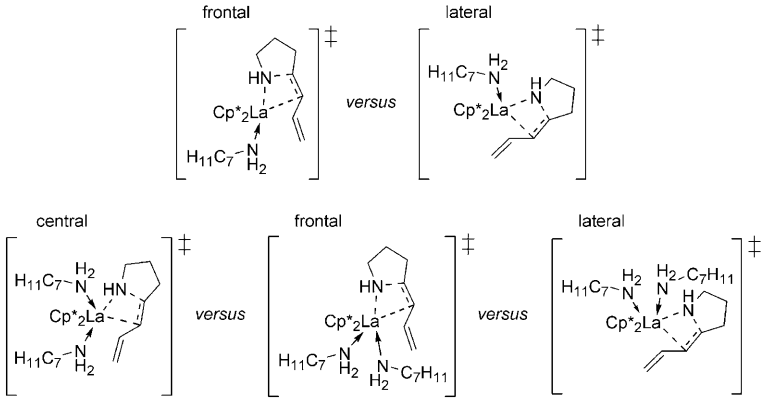

Scheme 6. Alternative trajectories for diene insertion into the La–N amido σ-bond in **3t**-S1 (top) and **3t**-S2 (bottom).

The most accessible path starts with dissociation of amine from **3**-S1 and insertive cyclisation to proceed in substrate-free species **3t**, **3c** through a four-centred TS structure that constitutes C^5–N bond formation with concomitant transformation of the *trans*/*cis* diene unit into a *syn*/*anti*-η^3-butenyl–La functionality. Noteworthy, the C^7=C^8 double bond associates closer to the lanthanide centre whilst traversing the TS, thereby playing a marked role in stabilising the TS structure (see Figure S4).[16] Following the reaction path further leads directly to **4s**, **4a** that has the azacycle coordinated by its N-donor centre and also by the *syn*/*anti*-η^3-butenyl tether to La. Isomers of **4** featuring a disrupted La–N linkage and/or a η^1-butenyl–La ligation are found to be at higher energy. Insertive cyclisation is facile connected with a moderate free energy of activation of 14.6 kcal mol^{-1} (**3t**-S1 → **3t** (+S) → **4s**)[17a] and 16.9 kcal mol^{-1} (**3t**-S1 → **3t** (+S) ⇄ **3c** → **4a**)[17a] and is somewhat uphill (Figure 5). The thermodynamic preference of the *trans*-diene **3t** isomer is seen to be essentially preserved in the TS structure and the La–azacycle intermediate **4s**. Given the distinct kinetic gap ($\Delta\Delta G^{\neq}$ = 6.6 kcal mol^{-1}, Figure 5) between **3t**-S1 → **3t** (+S) → **4s** and **3t**-S1 → **4s**-S1 paths, one can safely conclude that migratory diene insertion into the La–N σ-bond does occur in the substrate-free form of the La-amido catalyst complex, thereby corroborating previous findings.[4d]

Isomerisation of the allylic tether: An intriguing mechanistic aspect is as to whether **4s** and **4a** are in rapid equilibrium through facile isomerisation of the azacycle's butenyl tether. Isomer **4s** with a *syn*-η^3-butenyl–La tether is found to be predominantly formed by exocyclic ring closure on both kinetic and thermodynamic grounds, whilst **4a** is less populated. The most accessible pathway for butenyl–La tether isomerisation entails intramolecular η^3-π → η^1(C^6)-σ → η^3-π butenyl rearrangement and encounters a η^1(C^6)-σ-butenyl–La TS$_{ISO}$[**4**] that constitutes the rotation of the C^7=C^8 double bond around the formal C^6–C^7 single bond (see Tables S3a–S3c).[22–24] The barrier assessed for **4s** ⇄ **4a** conversion ($\Delta G^{\neq}$ = 22.7 kcal mol^{-1})[17a] is of similar magnitude as observed for related (η^3-allyl)$_3$–La complexes.[25,26] A somewhat higher free energy of activation is found for **4s**-S1 ⇄

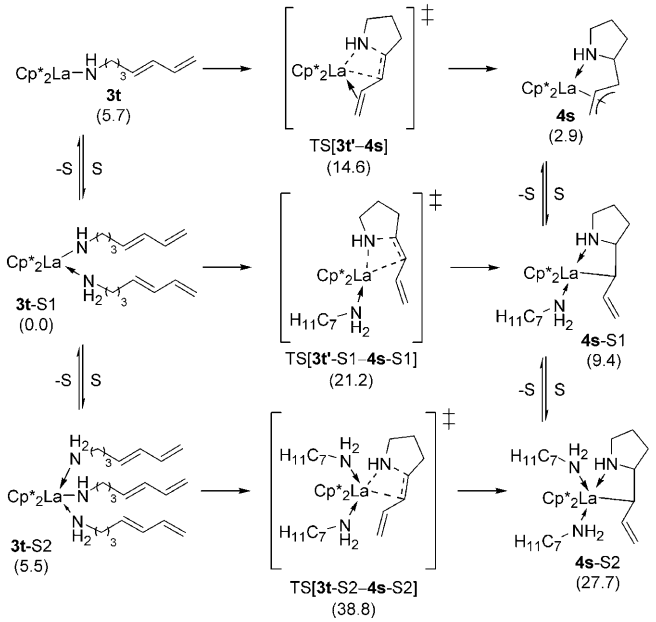

Figure 5. Most accessible pathways for diene insertion into the La–N amido σ-bond in substrate-free **3** and substrate adducts **3**-S1, **3**-S2.[17]

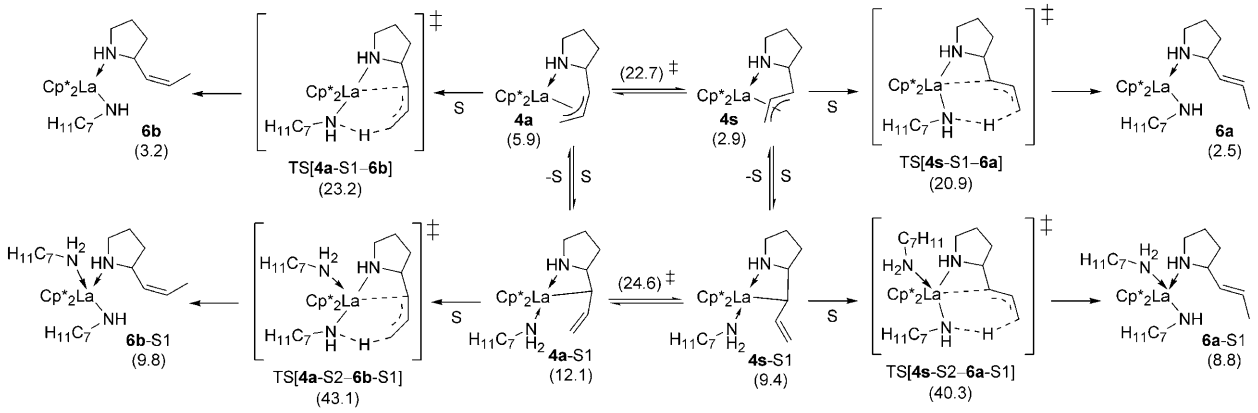

Figure 6. Most accessible pathways for protonation of the azacycle's tether in **4**.[17]

4a-S1 isomerisation, whilst a significantly higher absolute barrier would have to be overcome for isomerisation in **4**-S2. It indicates that isomerisation of the allylic tether does preferably occur in the substrate-free intermediate **4** and is kinetically more demanding than insertive cyclisation.

La–C azacycle aminolysis: Protonolysis at La–butenyl bonds entails initial complexation of a substrate molecule to **4s**, **4a**. It comes at the expense of the butenyl–La ligation; its mode switches from η^3 to η^1 (see Figure S7)[16] and **4s**-S1, **4a**-S1 adducts are uphill in free energy (see Table S4a in the Supporting Information). Aminolysis at La–butenyl(C^6) and La–butenyl(C^8) bonds evolves through a metathesis-like TS structure that constitutes the concomitant cleavage and formation of N–H and C–H bonds, respectively. This is accompanied by a butenyl → vinyl conversion, which is partially achieved in TS[**4s**-S1–**6a**] and TS[**4a**-S1–**6b**] (see Figure S7).[16] Notably, the order of *syn-anti* stability of **4** remains intact in the **4**-S1 adduct and also in the TS for La–butenyl(C^8) bond aminolysis (Figure 6). As a result, the most accessible aminolysis pathway via TS[**4s**-S1–**6a**] ($\Delta G^{\ddagger} = 20.9$ kcal mol^{-1}) furnishes **6a**, whilst the rival **4a** + **1t** → **6b** pathway is also traversable, but with a lower probability ($\Delta\Delta G^{\ddagger} = 2.3$ kcal mol^{-1}). Generation of **6a**, **6b** is essentially thermoneutral when commencing from **4s**, **4a**. Given that the N–H bond is more acidic than the C–H bond one expects a strong thermodynamic force for this transformation, the assessed modest reaction heat does, however, reflect the stability of the η^3-butenyl,η^1-*N*-azacycle–La ligation in **4s**, **4a**. Expulsion of pyrrolidine products through **6a**/**6b** + **1t** → **3t**-S1 + **P6a**/**P6b**, which is supposedly facile[27] and exergonic ($\Delta G = -8.1/-8.1$ kcal mol^{-1}), drives the overall aminolysis step further downhill. La–butenyl(C^8) bond aminolysis to commence from **4s**-S2, **4a**-S2 via various trajectories (Scheme 7) is found to invoke a substantially higher barrier (Figure 6) and can thus be safely discarded.

Several trajectories have been examined for La–butenyl(C^6) bond aminolysis.[16] The most accessible one features initial substrate association *cis* to the La–butenyl unit in **4s**, **4a** and has an activation barrier of 26.1 kcal mol^{-1} to overcome (see Table S4a in the SI). The distinct kinetic gap ($\Delta\Delta G^{\ddagger} = 5.2$ kcal mol^{-1}) relative to the most accessible pathways that furnishes **6a** (Figure 6) renders the **6c**-generating pathways almost impossible to traverse. In similarity to the findings above, aminolysis of the La-butenyl(C^6) linkage is kinetically impractical when commencing from **4s**-S2 or **4a**-S2 (see Table S4b)[16] and not compatible with the observed smooth catalysis.

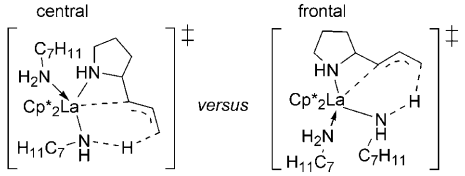

Scheme 7. Alternative trajectories for La–C^8 bond aminolysis commencing from **4s**-S2.

Comparison of mechanistic scenarios: Figure 7 collates the assessed Gibbs free-energy profiles for the most accessible pathways of all relevant steps for the alternative mechanistic scenarios described in Scheme 3 und 5. It reveals that intramolecular HA of aminodiene **1t** by the [Cp^*_2La–amido–(substrate)$_n$] catalyst species proceeds by migratory diene insertion into the La–N σ-bond and subsequent La–C azacycle aminolysis (Figure 7, right), thus the classical insertive mechanism[2a,b] prevails.

The formation of cycloamines in a single step[5] by non-insertive C–N ring closure with concomitant amino proton delivery onto the diene moiety (Figure 7, left) is seen to be unachievable. A direct pathway toward the observed **P6a**, **P6b** pyrrolidines appears to be non-existent, as indicated by the failure to locate a corresponding TS structure, because amino proton delivery at the distant terminal diene–C^8 centre does not polarise the diene–C^5 centre effectively toward nucleophilic amido attack. However, protonation at the adjacent diene–C^6 centre proved successful in this regard. This initially leads to **P6c** that could undergo complete conversion into **P6a**, **P6b** via cycloamine reinsertion and concomitant allyl isomerisation.[7a] Although observed in several cases, this scenario is impractical, because of the

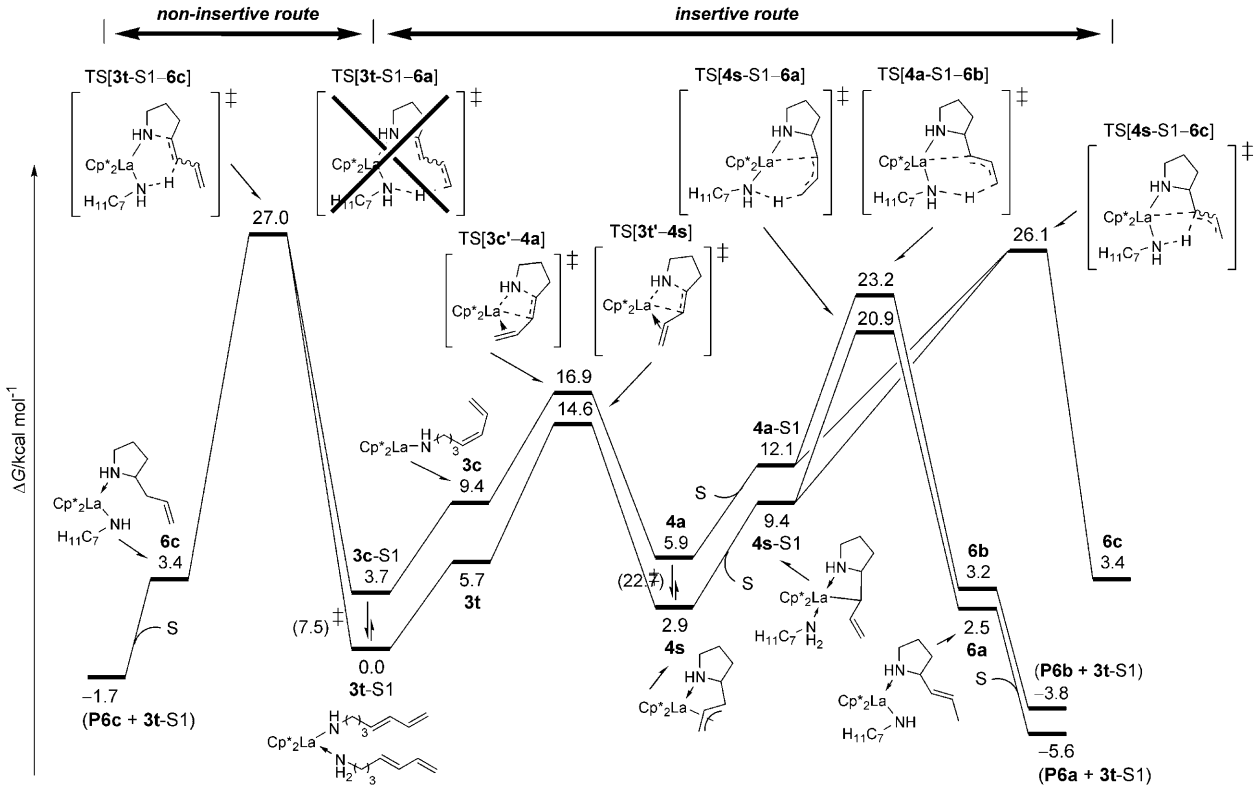

Figure 7. Condensed Gibbs free-energy profile for intramolecular hydroamination of aminodiene **1t** by the [Cp*$_2$La–amidodiene–(substrate)$_n$] catalyst species via alternative mechanistic paths. It focuses exclusively on the most accessible pathways for relevant steps. Pyrrolidine product liberation through **6a/6b/6c + 1t** → **P6a/P6b/P6c + 3t**-S1 is included.

prohibitive kinetic gap of 5.2 kcal mol^{-1} between the most accessible **P6a**- and **P6c**-generating pathways (Figure 7, right) and furthermore has been ruled out explicitly for the studied process by experiment.[7a] Hence, the non-insertive mechanism cannot account for the observed product spectrum.

Given that activation of the diene unit is distinctly different in the alternative mechanisms, the different response to steric encumbrance around the Ln centre is understandable. The stepwise Ln–N σ-bond insertive mechanism crucially relies on a Ln centre that is sufficiently accessible for the diene and allows furthermore a stabilising Ln–butenyl ligation in the azacycle intermediate. Insertive cyclisation (Figure 5) is seen to become significantly more demanding kinetically if an additional substrate molecule were to participate as a spectator. In contrast, a reduction of the lanthanide's accessibility has little impact on the non-insertive mechanisms, as indicated by the similar intrinsic barriers upon substrate association (Figure 4); in fact it tends to render it the favourable scenario. Considering the [Cp*$_2$La–amido–(substrate)$_2$] species **3**-S2 as a crude mimic of a catalyst with a protected lanthanide centre, DFT predicts that the non-insertive mechanism would prevail in such case (Figure 4–6). It should, however, be kept in mind that protection of the Ln centre, for instance by a suitably designed ligand architecture and/or a lanthanide with a smaller ionic radius, is unlikely to remove the electronically induced impracticability for ring closure and terminal diene–C[8] protonation to occur concomitantly. Hence, **P6c** is to expect as the kinetically controlled product, which can perhaps be transformed into **P6a**, **P6b** thereafter as described above.

In conclusion, the productive cycle of the Cp*$_2$La-mediated intramolecular HA of aminodienes comprises of the following steps: 1) rapid and reversible **3t**-S1 ⇄ **3t + 1t** displacement of the substrate from the catalyst resting state **3t**-S1; 2) facile and reversible **3t/3c** ⇄ **4s/4a** exocyclic diene insertion into the La–N(amido) σ-bond with ring closure; 3) rapid **4s/4a + 1t** ⇄ **4s**-S1/**4a**-S1 substrate association; and 4) subsequent turnover-limiting **4s**-S/**4a**-S → **6a/6b** aminolysis; 5) followed by **6a/6b + 1t** → **P6a/P6b + 3t**-S1 cycloamine expulsion. The following aspects are in support of this scenario: 1) the derived rate law is consistent with the observed empirical rate law;[4d] 2) the assessed effective barrier for turnover-limiting aminolysis ($\Delta G^{\ddagger}$ = 20.9 kcal mol^{-1}, Figure 7) agrees remarkably well with empirically determined Eyring parameters;[7b] and 3) the consistent elucidation of the ring-tether double-bond selectivity that correctly predicts the product distribution.[28]

Conclusions

Presented herein is a comprehensive computational examination of alternative scenarios for the intramolecular hydro-

amination of a prototypical aminodiene by a well-characterised lanthanocene–amido catalyst that are distinguished by how the amine-linked unsaturated C=C linkage is activated toward C–N ring closure. Firstly, the single-step transformation of an Ln–amidoolefin unit into a cycloamine through non-insertive cyclisation with concurrent amino proton delivery onto the olefin unit recently proposed by Scott has been explored and its key features have been described. This scenario has been compared with the stepwise insertive mechanism that involves 1) mobile substrate association/dissociation equilibrium for the **3t**-S1 resting state and for azacycle intermediates **4s**, **4a**; 2) facile and reversible exocyclic diene insertion into the La–N(amido) σ-bond; linked to 3) turnover-limiting La–C azacycle aminolysis. The classical Ln–N σ-bond insertive mechanism prevails for the studied intramolecular HA of (4*E*,6)-heptadienylamine **1t** by $[Cp^*_2La–CH(TMS)_2]$ starting material **2**. Support for this scenario comes from 1) the derived rate law that is consonant with the observed empirical rate law; 2) the remarkably good agreement of the assessed effective barrier for turnover-limiting aminolysis with empirically determined Eyring parameters; and 3) the consistent elucidation of the ring-tether double-bond selectivity that leads to correct predictions of the cycloamine distribution. On the other hand, the non-insertive mechanism is found to be not achievable and furthermore cannot account for the observed product spectrum for this particular lanthanocene–amido catalyst. As an important feature, outer-sphere cyclisation with concurrent amido proton delivery onto the terminal diene–C^8 centre appears to be non-existent, because it does not polarise the diene–C^5 centre sufficiently toward nucleophilic amido attack. Notwithstanding of these findings, the non-insertive mechanism cannot be discarded a priori for organolanthanide-mediated intramolecular aminodiene HA and can perhaps be operational for tailored catalyst designs featuring a less accessible lanthanide centre.

Spatial demands around the lanthanide centre effect the mechanistic scenarios differently. The Ln–N σ-bond insertive mechanism crucially relies on a sufficiently accessible lanthanide and greater encumbrance renders cyclisation in particular more demanding kinetically. In contrast, enhanced protection of the Ln centre, for example by well-designed ligand architectures and/or a lanthanide centre with a smaller ionic radius, influences the non-insertive cyclisation modestly and favours this mechanism. The present study indicates that the non-insertive mechanism would prevail if the lanthanide centre were to be protected effectively against C=C bond approach, whilst ensuring a high polarity of the Ln–N σ-bond together with a sufficiently acidic amino proton. Thus, the implementation of these general design principles is likely to advance a new generation of catalysts in the near future. However, a different product spectrum would be expected for aminodiene HA with ring closure proceeding in a insertive or non-insertive fashion.

The valuable, novel insights into the catalytic structure-reactivity relationships of aminodiene hydroamination mediated by organolanthanides disclosed in this study will likely assist the rational design of catalysts and facilitate further advances in the area.

Computational Methodology

All calculations based on Kohn–Sham density functional theory (DFT)[29] were performed by means of the program package TURBOMOLE[30] using the almost nonempirical *meta*-GGA Tao–Perdew–Staroverov–Scuseria (TPSS) functional[31] within the RI-*J* integral approximation[32] in conjunction with flexible basis sets of triple-ζ quality. For La we used the Stuttgart–Dresden scalar-relativistic pseudopotential (SDD, 46 core electrons)[33] in combination with the (7s7p5d1f)/[6s4p3d1f] (TZVPext) valence basis set.[34] This pseudopotential treats $[Kr]4d^{10}4f^0$ as a fixed core, whereas $5s^25p^66\,s^25d^16p^0$ shells are taken into account explicitly. All remaining elements were represented by Ahlrich's valence triple-ζ TZVP basis set[35] with polarization functions on all atoms. The energy landscape of the entire cyclohydroamination course was assessed for (4*E*,6)-heptadienylamine (**1t**) together with $[Cp^*_2La–amidodiene–(substrate)_n]$ as the catalyst complex. No structural simplification of any of the involved key species was imposed. The DFT calculations have simulated the authentic reaction conditions by treating the bulk effects of the benzene solvent by a consistent polarisable continuum model.[36] All the stationary points were fully located with inclusion of solvation. Frequency calculations were performed to confirm the nature of all optimised key structures and to determine thermodynamic parameters (298 K, 1 atm) under the rigid-rotor and harmonic approximations. The mechanistic conclusions drawn in this study were based on the Gibbs free-energy profile of the entire catalytic cycle assessed at the TPSS(COSMO)/SDD+TZVP level of approximation for experimental condensed phase conditions. The analysis of the bonding situation was performed with the aid of Wiberg bond orders (WBO)[37] that are known to provide a good measure of the covalent bond order between two interacting atoms. Natural population analyses (NPA)[38] were performed with the NBO[39] in conjunction with the MAG-ReSpect[40] module. Further details together with a description of the employed computational methodology are given in the Supporting Information. Calculated structures were visualised by employing the StrukEd program,[41] which was also used for the preparation of 3D molecule drawings.

Acknowledgements

The author wishes to thank Professor Malkin (Slovak Academy of Sciences, Bratislava, Slovakia) and Professor Kaupp (University of Würzburg, Germany) for making the MAG-ReSpect module available to us and also Professor Helgaker (University of Oslo, Norway) for permission to use some of the DALTON routines.

[1] For reviews of catalytic hydroamination, see: a) L. S. Hegedus, *Angew. Chem.* **1988**, *100*, 1147; *Angew. Chem. Int. Ed.* **1998**, *37*, 1113; b) D. M. Roundhill, *Catal. Today* **1997**, *37*, 155; c) T. E. Müller, M. Beller, *Chem. Rev.* **1988**, *88*, 675; d) M. Nobis, B. Drießen-Hölscher, *Angew. Chem.* **2001**, *113*, 4105; *Angew. Chem. Int. Ed.* **2001**, *40*, 3983; e) R. Taube in *Applied Homogeneous Catalysis with Organometallic Complexes* (Eds.: B. Cornils, W. A. Herrmann), Wiley-VCH, Weinheim, **2002**, pp. 513–524; f) F. Seayad, A. Tillack, C. G. Hartung, M. Beller, *Adv. Synth. Catal.* **2002**, *344*, 795; g) G. A. Molander, J. A. C. Romero, *Chem. Rev.* **2002**, *102*, 2161; h) F. Pohlki, S. Doye, *Chem. Soc. Rev.* **2003**, *32*, 104; i) P. W. Roesky, T. E. Müller, *Angew. Chem.* **2003**, *115*, 2812; *Angew. Chem. Int. Ed.* **2003**, *42*, 2708; j) J. F. Hartwig, *Pure Appl. Chem.* **2004**, *76*, 507; k) S. Hong, T. J. Marks, *Acc. Chem. Res.* **2004**, *37*, 673; l) K. C. Hultzsch, *Adv. Synth. Catal.* **2005**, *347*, 367; m) A. L. Odom, *Dalton Trans.* **2005**, 225; n) R. Severin, S. Doye, *Chem. Soc. Rev.* **2007**, *36*, 1407; o) I. Aillaud, J. Collin, J. Hannedouche, E. Schulz, *Dalton Trans.*

2007, 5105; p) J. F. Hartwig, *Nature* **2008**, *455*, 314; q) T. E. Müller, K. C. Hultzsch, M. Yus, F. Foubelo, M. Tada, *Chem. Rev.* **2008**, *108*, 3795.

[2] For cyclohydroamination mediated by organolanthanides, see: a) M. R. Gagné, T. J. Marks, *J. Am. Chem. Soc.* **1989**, *111*, 4108; b) M. R. Gagné, T. J. Marks, *J. Am. Chem. Soc.* **1992**, *114*, 275; c) Y. Li, P.-F. Fu, T. J. Marks, *Organometallics* **1994**, *13*, 439; d) Y. Li, T. J. Marks, *J. Am. Chem. Soc.* **1996**, *118*, 9295; e) G. A. Molander, E. D. Dowdy, *J. Org. Chem.* **1998**, *63*, 8983; f) M. R. Bürgstein, H. Berberich, P. W. Roesky, *Organometallics* **1998**, *17*, 1452; g) V. M. Arredondo, F. E. McDonald, T. J. Marks, *Organometallics* **1999**, *18*, 1949; h) A. T. Gilbert, B. L. Davis, T. J. Emge, R. D. Broene, *Organometallics* **1999**, *18*, 2125; i) G. A. Molander, E. D. Dowdy, *J. Org. Chem.* **1999**, *64*, 6515; j) Y. K. Kim, T. Livinghouse, J. E. Bercaw, *Tetrahedron Lett.* **2001**, *42*, 2944; k) G. A. Molander, E. D. Dowdy, S. K. Pack, *J. Org. Chem.* **2001**, *66*, 4344; l) M. R. Bürgstein, H. Berberich, P. W. Roesky, *Chem. Eur. J.* **2001**, *7*, 3078; m) S. Hong, T. J. Marks, *J. Am. Chem. Soc.* **2002**, *124*, 7886; n) S. Hong, S. Tian, M. V. Metz, T. J. Marks, *J. Am. Chem. Soc.* **2003**, *125*, 14768; o) A. Zulys, T. K. Panda, M. T. Gamer, P. W. Roesky, *Chem. Commun.* **2004**, 2584; p) J.-S. Ryu, T. J. Marks, F. E. McDonald, *J. Org. Chem.* **2004**, *69*, 1038; q) A. M. Seyam, B. D. Stubbert, T. R. Jensen, J. J. O'Donnell III, C. L. Stern, T. J. Marks, *Inorg. Chim. Acta* **2004**, *357*, 4029; r) J. Collin, J.-C. Daran, O. Jacquet, E. Schulz, A. Trifonov, *Chem. Eur. J.* **2005**, *11*, 3455.

[3] For some leading references, see: a) A. L. Casalnuovo, J. C. Calabrese, D. Milstein, *Inorg. Chem.* **1987**, *26*, 971; b) T. E. Müller, A.-K. Pleier, *J. Chem. Soc. Dalton Trans.* **1999**, 583; c) T. E. Müller, M. Grosche, E. Herdtweck, A.-K. Pleier, E. Walter, Y.-K. Yan, *Organometallics* **2000**, *19*, 170; d) T. Kondo, T. Okada, T. Suzuki, T. Mitsudo, *J. Organomet. Chem.* **2001**, *622*, 149; e) S. Burling, L. D. Field, B. A. Messerle, P. Turner, *Organometallics* **2004**, *23*, 1714; f) L. M. Lutete, I. Kadota, Y. Yamamoto, *J. Am. Chem. Soc.* **2004**, *126*, 1622; g) L. D. Field, B. A. Messerle, K. Q. Vuong, P. Turner, *Organometallics* **2005**, *24*, 4241; h) G. B. Bajracharya, Z. Huo, Y. Yamamoto, *J. Org. Chem.* **2005**, *70*, 4883; i) Ch. F. Bender, R. A. Widenhoefer, *J. Am. Chem. Soc.* **2005**, *127*, 1070; j) D. Karshtedt, A. T. Bell, T. D. Tilley, *J. Am. Chem. Soc.* **2005**, *127*, 12640; k) X. Li, A. R. Chianese, T. Vogel, R. H. Crabtree, *Org. Lett.* **2005**, *7*, 5437; l) F. E. Michael, B. M. Cochran, *J. Am. Chem. Soc.* **2006**, *128*, 4246; m) A. Takemiya, J. F. Hartwig, *J. Am. Chem. Soc.* **2006**, *128*, 6042; n) N. T. Patil, L. M. Lutete, H. Wu, N. K. Pahadi, I. D. Gridnev, Y. Yamamoto, *J. Org. Chem.* **2006**, *71*, 4270; o) J. Zhou, J. F. Hartwig, *J. Am. Chem. Soc.* **2008**, *130*, 12220; p) J. L. McBee, A. T. Bell, T. D. Tilley, *J. Am. Chem. Soc.* **2008**, *130*, 16562; q) C. Munro-Leighton, S. A. Delp, N. M. Alsop, E. D. Blue, T. B. Gunnoe, *Chem. Commun.* **2008**, 111; r) B. M. Cochran, F. E. Michael, *J. Am. Chem. Soc.* **2008**, *130*, 2786.

[4] For computational studies of organolanthanide-assisted intramolecular HA of various substrate classes, see: aminoalkene substrates: a) A. Motta, G. Lanza, I. L. Fragala, T. J. Marks, *Organometallics* **2004**, *23*, 4097; aminoalkyne substrates: b) A. Motta, G. Lanza, I. L. Fragala, T. J. Marks, *Organometallics* **2006**, *25*, 5533; aminoallene substrate: c) S. Tobisch, *Chem. Eur. J.* **2006**, *12*, 2520; aminodiene substrates: d) S. Tobisch, *J. Am. Chem. Soc.* **2005**, *127*, 11979; e) S. Tobisch, *Chem. Eur. J.* **2007**, *13*, 9127.

[5] L. E. Allan, D. J. Fox, R. J. Deeth, A. L. Gott, P. Scott, *Proceedings of the 42nd IUPAC Congress*, Glasgow, UK, August 2–7, 2009.

[6] A possible explanation for the observed KIE in aminoalkene HA in the context of the La–N σ-bond insertive mechanism with turnover-limiting cyclisation is given in reference [2b]. Note that the rate-limiting step of the insertive mechanism is not identical for the various substrate classes; cyclisation is the rate-limiting event for aminoalkenes/-alkynes (ref. [4a,b]), whereas for aminoallenes/-dienes protonolysis is turnover limiting (ref. [4c,d])

[7] a) S. Hong, A. M. Kawaoka, T. J. Marks, *J. Am. Chem. Soc.* **2003**, *125*, 15878; b) The following Eyring parameters have been determined empirically for intramolecular HA of **1t** with [Cp^*_2La–$CH(TMS)_2$] precatalyst **2**: $\Delta H^{\ddagger} = 10.4\ kcal\,mol^{-1}$, $\Delta S^{\ddagger} = -32.7\ cal\,K^{-1}\,mol^{-1}$, $\Delta G^{\ddagger} = 20.1\ kcal\,mol^{-1}$ (RT); reference [7a]; see also references [2n and 2m].

[8] P. A. Hunt, *Dalton Trans.* **2007**, 1743.

[9] For computational studies of Group 4 transition-metal-assisted intramolecular HA of various substrate classes, see: aminoalkene substrates: a) C. Müller, R. Koch, S. Doye, *Chem. Eur. J.* **2008**, *14*, 10430; aminoallene substrates: b) S. Tobisch, *Dalton Trans.* **2006**, 4277; c) S. Tobisch, *Chem. Eur. J.* **2007**, *13*, 4884; d) S. Tobisch, *Chem. Eur. J.* **2008**, *14*, 8590.

[10] For computational studies of transition metal- and organolanthanide-assisted intermolecular HA, see: a) H. M. Senn, P. E. Blöchl, A. Togni, *J. Am. Chem. Soc.* **2000**, *122*, 4098; b) B. F. Straub, R. G. Bergman, *Angew. Chem.* **2001**, *113*, 4768; *Angew. Chem. Int. Ed.* **2001**, *40*, 4632; c) S. Tobisch, *Chem. Eur. J.* **2005**, *11*, 6372; d) C. A. Tsipis, C. E. Kefalidis, *J. Organomet. Chem.* **2007**, *692*, 5245.

[11] For a computational study of organoactinide-assisted intramolecular HA of aminodienes see: S. Tobisch, *Chem. Eur. J.* **2010**, *16*, 3441.

[12] For a computational study of late transition-metal assisted HA of aminoalkenes, see: K. D. Hesp, S. Tobisch, M. Stradiotto, *J. Am. Chem. Soc.* **2010**, *132*, 413.

[13] The data presented herein for the lanthanocene–amido catalyst species and relevant steps of the Ln–N σ-bond insertive mechanism can deviate somewhat from the ones reported in reference [4d] on the identical catalyst system, which used a different (BP86) DFT method. The present study can be regarded as being superior, because of the applied state-of-the-art methodology that involves a more consistent treatment of the authentic reaction conditions, together with the usage of the modern, almost nonempirical, well-performing *meta*-GGA TPSS functional, as detailed in the computational methodology section.

[14] The notation of key structures has been chosen according to reference [4d].

[15] Substrate association and dissociation steps are known to be facile in organolanthanide-mediated intramolecular hydroamination. For NMR evidence of rapid association/dissociation of free amine and of amido/amine permutation see reference [2b].

[16] See the Supporting Information for more detail.

[17] a) The prevalent [Cp^*_2La–amidodiene–substrate] form **3t**-S1 of the La–amido catalyst complex (with the appropriate number of substrate molecules) has been chosen as reference for relative free energies. b) Only the most accessible pathways are shown; see the SI for a complete account of all the studied pathways.

[18] The cut-off for drawing La–C bonds was arbitrarily set to 3.1 Å. The hydrogen atoms on the methyl groups of the Cp^*_2La backbone are omitted for the sake of clarity. Note that the amino-/amidodiene units are displayed in a truncated fashion for several of the species.

[19] The structure on the right does not constitute a true TS structure for non-insertive cyclisation with concurrent proton delivery onto diene–C[8], but a tentative structure for **3t**-S2 → **6a**-S1 transformation in a single step. Notably, the corresponding TS structure could not be located (see the text).

[20] The is ample precedence for η^3-allylic structures in organo-4f-element chemistry; see for instance: a) G. Jeske, H. Lauke, H. Mauermann, P. N. Swepston, H. Schumann, T. J. Marks, *J. Am. Chem. Soc.* **1985**, *107*, 8091; b) E. Bunell, B. J. Burger, J. E. Bercaw, *J. Am. Chem. Soc.* **1988**, *110*, 976; c) S. P. Nolan, C. L. Stern, T. J. Marks, *J. Am. Chem. Soc.* **1989**, *111*, 7844; d) W. J. Evans, T. A. Ulibarri, J. W. Ziller, *J. Am. Chem. Soc.* **1990**, *112*, 2314; e) A. Scholz, A. Smola, J. Scholz, J. Löbel, H. Schimann, K.-H. Thiele, *Angew. Chem.* **1991**, *103*, 444; *Angew. Chem. Int. Ed. Engl.* **1991**, *30*, 435; f) R. Taube, H. Windisch, F. Görlitz, H. Schumann, *J. Organomet. Chem.* **1993**, *445*, 85; g) W. J. Evans, R. A. Keyer, G. W. Rabe, D. K. Drummond, J. W. Ziller, *Organometallics* **1993**, *12*, 4664; h) W. J. Evans, S. L. Gonzales, J. W. Ziller, *J. Am. Chem. Soc.* **1994**, *116*, 2600; i) R. Taube, H. Windisch, H. Hemling, H. Schumann, *J. Organomet. Chem.* **1998**, *555*, 201; j) R. Taube, St. Maiwald, J. Sieler, *J. Organomet. Chem.* **2001**, *621*, 327.

[21] a) M. R. Gagné, L. Brard, V. P. Conticello, M. A. Giardello, C. L. Stern, T. J. Marks, *Organometallics* **1992**, *11*, 2003; b) M. A. Giardel-

lo, V. P. Conticello, L. Brard, M. Sabat, A. L. Rheingold, C. L. Stern, T. J. Marks, *J. Am. Chem. Soc.* **1994**, *116*, 10212; c) M. R. Douglass, M. Ogasawa, S. Hong, M. V. Metz, T. J. Marks, *Organometallics* **2002**, *21*, 283.

[22] J. Lukas, P. W. N. M. van Leeuwen, H. C. Volger, A. P. Kouwenhoven, *J. Organomet. Chem.* **1973**, *47*, 153.

[23] a) J. W. Faller, M. E. Thomsen, M. J. Mattina, *J. Am. Chem. Soc.* **1971**, *93*, 2642; b) K. Vrieze, *Fluxional Allyl Complexes in Dynamic Nuclear Magnetic Resonance Spectroscopy* (Eds.: L. Jackmann, F. A. Cotton), Academic Press, New York, **1975**.

[24] S. Tobisch, R. Taube, *Organometallics* **1999**, *18*, 3045.

[25] a) R. Taube, H. Windisch, *J. Organomet. Chem.* **1994**, *472*, 71; b) R. Taube, H. Windisch, St. Maiwald, H. Hemling, H. Schuhmann, *J. Organomet. Chem.* **1996**, *513*, 49.

[26] The free-energy of activation for allylic isomerisation has been determined by NMR spectroscopy to be about 16 kcal mol^{-1} for [(η^5-Cp′)La(η^3-C_3H_5)$_3$]$^-$ compounds with Cp′ = C_5H_5, C_5Me_5 (ref. [26a]) and to be >15.5 kcal mol^{-1} for the [La(η^3-C_3H_5)$_3$] dioxane adduct (ref. [26b]). It compares favourably with the intrinsic **4s** → TS_{ISO}[**4**] → **4a** barrier (i.e., relative to **4s**) of 19.8 kcal mol^{-1}.

[27] Examination by a linear-transit approach gave no indication that this process is associated with a significant enthalpy barrier.

[28] In brief, the assessed barriers of 20.9/23.2/26.1 kcal mol^{-1} (Figure 7) for the most accessible pathways of the selectivity-determining and turnover-limiting aminolysis that leads to **P6a**/**P6b**/**P6c** corresponds to a **P6a**:**P6b**:**P6c** ratio of 98:2:0 (298.15 K) upon application of Stefan–Boltzmann statistics. A more detailed analysis can be found in reference [4d].

[29] R. G. Parr, W. Yang, *Density-Functional Theory of Atoms and Molecules*, Oxford University Press, New York, **1989**.

[30] a) R. Ahlrichs, M. Bär, M. Häser, H. Horn, C. Kölmel, *Chem. Phys. Lett.* **1989**, *162*, 165; b) O. Treutler, R. Ahlrichs, *J. Chem. Phys.* **1995**, *102*, 346; c) TURBOMOLE, version 5.9, R. Ahlrichs, F. Furche, C. Hättig, W. Klopper, M. Sierka, F. Weigend, University of Karlsruh, Karlsruhe (Germany), **2006**, http://www.turbomole.com.

[31] a) P. A. M. Dirac, *Proc. Royal Soc. London Ser. A* **1929**, *123*, 714; b) J. C. Slater, *Phys. Rev.* **1951**, *81*, 385; c) J. P. Perdew, Y. Wang, *Phys. Rev. B* **1992**, *45*, 13244; d) J. Tao, J. P. Perdew, V. N. Staroverov, G. E. Scuseria, *Phys. Rev. Lett.* **2003**, *91*, 146401; e) J. P. Perdew, J. Tao, V. N. Staroverov, G. E. Scuseria, *J. Chem. Phys.* **2004**, *120*, 6898.

[32] a) O. Vahtras, J. Almlöf, M. W. Feyereisen, *Chem. Phys. Lett.* **1993**, *213*, 514; b) K. Eichkorn, O. Treutler, H. Öhm, M. Häser, R. Ahlrichs, *Chem. Phys. Lett.* **1995**, *242*, 652.

[33] M. Dolg, H. Stoll, A. Savin, H. Preuß, *Theor. Chim. Acta* **1989**, *75*, 173.

[34] a) F. Weigend, R. Ahlrichs, *Phys. Chem. Chem. Phys.* **2005**, *7*, 3297; b) F. Weigend, *Phys. Chem. Chem. Phys.* **2006**, *8*, 1057.

[35] a) A. Schäfer, C. Huber, R. Ahlrichs, *J. Chem. Phys.* **1994**, *100*, 5829; b) K. Eichkorn, F. Weigend, O. Treutler, R. Ahlrichs, *Theor. Chem. Acc.* **1997**, *97*, 119.

[36] a) A. Klamt, G. Schüürmann, *J. Chem. Soc. Perkin Trans. 2* **1993**, 799; b) A. Klamt in *Encyclopedia of Computational Chemistry, Vol. 1* (Ed.: P. von R. Schleyer), Wiley, New York, **1998**, pp. 604–615.

[37] K. B. Wiberg, *Tetrahedron* **1968**, *24*, 1083.

[38] A. E. Reed, R. B. Weinstock, F. Weinhold, *J. Chem. Phys.* **1985**, *83*, 735.

[39] NBO 4M, E. D. Glendening, J. K. Badenhoop, A. E. Reed, J. E. Carpenter, F. Weinhold, Theoretical Chemistry Institute, University of Wisconsin, Madison, **1999**.

[40] ReSpect program, version 1.2, V. G. Malkin, O. L. Malkina, R. Reviakine, A. V. Arbuznikov, M. Kaupp, B. Schimmelpfennig, I. Malkin, M. Repiský, S. Komorovský, P. Hrobarik, E. Malkin, T. Helgaker, K. Ruud, **2005**.

[41] For further details, see: http://www.struked.de.

Received: May 18, 2010
Published online: October 11, 2010

